Journal of Solid State Chemistry **144,** 318–324 (1999)
Article ID jssc.1999.8151, available online at http://www.idealibrary.com on IDEAL®

Characterization of a New Organic-Cation Cyclotetraphosphate: $(1,4\text{-}HOC_6H_4NH_3)_4P_4O_{12} \cdot 6H_2O$

E. H. Soumhi,*[,1] I. Saadoune,* A. Driss,† and T. Jouini†

*Département de Chimie, Université Cadi Ayyad, FST-Marrakech, B.P. 618, Marrakech, Morrocco; and †Faculté des Sciences de Tunis, Département de Chimie, Campus Universitaire, 1060 Tunis, Tunisia

Received September 21, 1998; in revised form December 18, 1998; accepted December 30, 1998

The tetra(*para*-phenolammonium)cyclotetraphosphate hexahydrate, $(1,4\text{-}HOC_6H_4NH_3)_4P_4O_{12}\cdot 6H_2O$ ($M = 864.51$ g mol^{-1}), is monoclinic $P2_1/c$ with the unit cell parameters $a = 9.836(2)$ Å, $b = 8.591(1)$ Å, $c = 22.769(5)$ Å, $\beta = 95.41(2)^\circ$. The structure of this compound can be described as a succession of inorganic and organic sheets parallel to the (001) plane. The existence of the OH and NH_3 groups in position *para* to the organic cation leads to the cohesion of the inorganic sheets, forming a three-dimensional network.The IR spectrum of $(1,4\text{-}HOC_6H_4NH_3)_4P_4O_{12}\cdot 6H_2O$ is reported and discussed according to the theoretical group analysis. The IR data confirm the atomic arrangement within the structure. The coupled TG–DTA thermal study shows the successive departure of four and two water molecules, confirming the hydrated character of this cyclophosphate. © 1999 Academic Press

INTRODUCTION

The condensed phosphates resulting from interaction between phosphoric acid and organic molecules, such as amines aminoalcohols, and amino acids, have been extensively studied by several groups (1–10). The attention paid to these materials increased greatly approximately a decade ago when it was established that these compounds could present peculiar physicochemical properties.

In fact, it has been demonstrated that some organic-cation phosphates have good protonic conduction, and thus are of interest as solid electrolytes (11). Furthermore, research on these phases was stimulated by their possible utilization in the nonlinear optic domain (12, 13). Nevertheless, the research efforts were essentially devoted to the synthesis and structure of new materials. A main part of these studies has been concerned with inorganic phosphates (14, 15), but a few organic-cation phosphates have been described (16, 17).

In the present paper, we report a detailed structural investigation of a new organic cyclotetraphosphate with a bifunctional *para*-phenolammonium cation, $1,4\text{-}HOC_6H_4NH_3)_4P_4O_{12}\cdot 6H_2O$. In addition, this nominal compound has been characterized by thermal analysis and IR spectroscopy.

EXPERIMENTAL

The tetra(*para*-phenolammonium)cyclotetraphosphate hexahydrate $(1,4\text{-}HOC_6H_4NH_3)_4P_4O_{12}\cdot 6H_2O$ has been prepared by the procedure utilized for other analogous phosphates having organic cations (18–21). This preparation is achieved in several steps: the starting cyclotetraphosphate acid $H_4P_4O_{12}$ is obtained by passing a concentrated solution of hydrated sodium cyclotetraphosphate acid salt $Na_4P_4O_{12}\cdot 4H_2O$ through a column containing an Amberlite IR 120 type ion exchange resin. Because of its instability, the obtained acid is rapidly neutralized with *para* phenolamine solution. After this step, the resulting solution is filtered and exposed to air until small colorless plates of $(1,4\text{-}HOC_6H_4NH_3)_4P_4O_{12}\cdot 6H_2O$ appeared.

Main crystal features and all the experimental parameters used for the X-ray diffraction data collection and for the structural determination and its final results are summarized in Table 1.

Thermal analysis measurements are performed at a heating rate of 5°/min using a SETARAM TG-ATD 92 thermoanalyzer. The infrared spectra were recorded with a Perkin–Elmer IR-983 Cr spectrometer in KBr tablets.

RESULTS AND DISCUSSION

1. *Structure Description*

As reported in Table 1, the nominal compound crystallizes in the monoclinic system, space group $P2_1/c$, with the monoclinic unit cell parameters $a = 9.836(2)$ Å, $b = 8.591(1)$ Å, $c = 22.769(5)$ Å, $\beta = 95.41(2)^\circ$. From a general point of view, this phosphate could be described as a layered

---

[1] To whom correspondence should be addressed.

0022-4596/99 $30.00

structure consisting a alternating organic and inorganic sheets along the [001] direction. One can assume that this atomic arrangement is characteristic of this family of phosphates (18–20). The projection of the structure along the **b** axis is given in Fig. 1, and the fractional atomic coordinates are summarized in Table 2.

a. Inorganic group. The inorgnic sheet is formed simultaneously by the cyclotetraphosphate anions $[P_4O_{12}]^{4-}$ and the water molecules alternating along the [100] direction as shown in Fig. 2. The cyclotetraphosphate anion is, as usual, make up of a ring of four PO_4 tetrahedra sharing corners. It is centrosymmetric and exhibits only two independent PO_4 tetrahedra. It presents a strong distortion as shown by the P–P–P angle values of 83° and 97° (Table 3). Note that the sum of these angle values is 180°, in good agreement with earlier results concerning $[P_4O_{12}]^{4-}$ groups having C_i local symmetry. It should be noticed that these angle values are close to those observed in $(C_6H_{18}N_2)_2P_4O_{12}\cdot 4H_2O$ phosphate (18). Furthermore, the P–O distances within the tetrahedra of the P_4O_{12} ring vary from 1.473(2) to 1.607(2) Å, while the O–P–O angle values vary from 99.37(9) to 120.9(1)°. Such values agree with those previously reported for other studied cyclotetraphosphates (16).

The water molecules, which are interconnected as triplets labeled $(OW_1 \leftarrow OW_2 \leftarrow OW_3)$, are also intercalated between the $[P_4O_{12}]^{4-}$ cycles, forming infinite sheets parallel to the **ab** plane. Each triplet is oriented to only one P_4O_{12} ring, with which it forms two H bonds. Thus, the P_4O_{12} rings are not interconnected. Nevertheless, the water molecules play an important role in structure cohesion. Effectively, the water molecules participate in 9 H bonds out of 14 establised in the asymmetrical unit.

b. Organic group. The atomic agreement contains two independent $(HOC_6H_4NH_3)^+$ cations which are parallel through with opposite orientations. A similar geometric characteristic of this bifunctional organic cation, reported in Table 3, has been evidenced in other phosphates containing the same organic cation (19–21). The organic groups are not directly connected. Since these organic cations are bifunctional (NH_3 and OH in *para* positions), they interact, by hydrogen bonds, with the inorganic groups belonging to two adjacent sheets. Thus, the interaction between the inorganic and organic groups leads to two-dimensional cohesion of the inorganic sheets and thus to a 3D hydrogen bond system.

As reported in Table 4, the structure contains 14 hydrogen bonds. Of these 2, involving the hydroxyl group of the

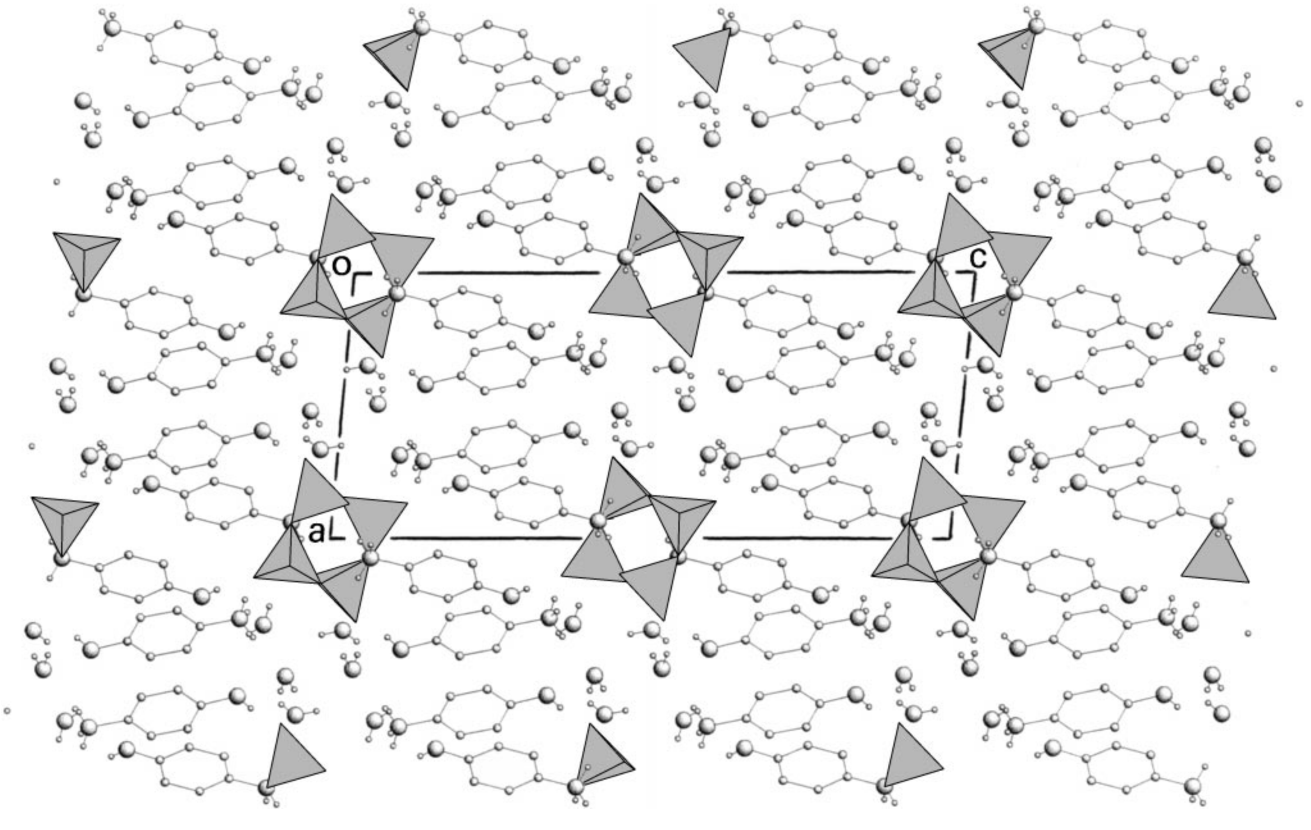

FIG. 1. Projection along the *b* axis of the $(1,4\text{-}HOC_6H_4NH_3)_4P_4O_{12}\cdot 6H_2O$ structure.

TABLE 1

Main Crystallographic Features, Parameters Used for the X-Ray Data Collection, Strategy Used for the Crystal Structure Determination, and Its Final Results

Crystal Data	
$C_{24}H_{32}N_4P_4O_{12} \cdot 6H_2O$	Mo$K\alpha$ radiation
$M = 864.51$ g mol^{-1}	$\lambda = 0.71069$ Å
Monoclinic	Cell parameters from 25 reflections
$P2_1/c$	$\theta = 10.5$–$16.5°$
$a = 9.836(2)$ Å	$\mu = 0.286$ mm^{-1}
$b = 8.591(1)$ Å	$T = 298$ K
$c = 22.769(5)$ Å	Small plate
$\beta = 95.41(2)°$	Dimens: $0.13 \times 0.3 \times 0.8$ mm
$V = 1915.4(6)$ Å^3	
$Z = 2$	Colorless
$D_x = 1.499$ mg m^{-3}	
$D_m \cdot$ not measured	
Data Collection	
Enraf–Nonius CAD-4 Diffractometer (28)	$R_{int} = 0.0148$
$\omega/2\theta$ scans	$\theta_{max} = 26.97°$
Absorption correction: none	$h, -12 \rightarrow 12$; k, 0 + 10; 1,0 + 29
4280 measured reflections	1 standard reflection every 120 mn
4171 indepenent reflections	
3149 observed reflections: $I > 2\sigma(I)$	Intensity decay: 1.5%
Refinement	
Refinement on F^2	$(\Delta/\sigma)_{max} < 10^{-3}$
$R(F^2 > 2\sigma(F^2)) = 0.0415$	$\Delta\rho_{max} = 0.317$ e Å^{-3}
$wR(F^2) = 0.0962$	$\Delta\rho_{min} = -0.277$ e Å^{-3}
$S = 1.112$	Extinction correction: ShelxL93 (30, 31)
4171 reflections	Extinction coefficient: 0.013(1)
333 parameters	
All **H** atoms refined	
$w = 1/[\sigma^2(F_0^2) + (0.0493P)^2 + 0.9173P]$ where $P = (F_0^2 + 2F_c^2)/3$	Scattering factors from "International Tables for Crystallography" (Vol. C)

organic cation and the external oxygen of P_4O_{12} ring, are strong: $d_{O_1\text{-}O_{11}} = 2.684$ Å and $d_{O_2\text{-}O_{12}} = 2.648$ Å. The 12 remaining hydrogen bonds are weak. Their corresponding N(O)---O distances are between 2.743 and 3 Å (22–23).

2. *IR Spectroscopy*

The IR spectrum of $(1,4\text{-}HOC_6H_4NH_3)_4P_4O_{12} \cdot 6H_2O$ phosphate is illustrated in Fig. 3. As mentioned above, this phosphate crystallizes in the $P2_1/c$ space group. The P_4O_{12} cycles occupy a crystallogaphic site having C_i symmetry. According to the theoretical group analysis, the number of normal modes is 42, given by the reduced representation: $\Gamma_{int.} = 21A_g + 21A_u$. Only the A_u modes are active in the IR spectroscopy. These 21 IR-active modes could be divided into 8 stretching modes and 13 deformation modes.

With the aim of attributing each band, Table 5 compares our result with the observed and calculated wavenumbers in the case of C_{2h} symmetry of P_4O_{12} cycle (24), and our result with those observed in the $(NH_2NH_3)_4P_4O_{12}$ phosphate, in which the P_4O_{12} cycle have the same C_i local symmetry (25).

TABLE 2

Atoms	x	y	z	U_{eq} (Å^2)
(a) Fractional Atomic Coordinates and Equivalent Isotropic Displacement Parameters for Non H atoms; $U_{eq.} = \frac{1}{3}\sum_i\sum_j U_{ij}a_i^*a_j^*\mathbf{a}_i\mathbf{a}_j$				
P1	0.17552(5)	0.10088(6)	0.01978(2)	0.0311(2)
P2	−0.08877(6)	0.14059(6)	0.06755(2)	0.0313(2)
O11	0.3108(2)	0.1083(2)	0.05429(8)	0.0471(4)
O21	0.1341(2)	0.2198(2)	−0.02495(7)	0.0439(4)
OL12	0.0658(2)	0.0852(2)	0.06711(6)	0.0402(4)
OL21	0.1643(2)	−0.0710(2)	−0.00809(6)	0.0400(4)
O12	−0.1415(2)	0.0664(2)	0.11939(6)	0.0446(4)
O22	−0.0970(2)	0.3126(2)	0.06179(7)	0.0425(4)
OW1	−0.3194(3)	0.4887(3)	0.0970(1)	0.0699(6)
OW2	−0.3411(3)	0.0606(3)	0.4681(1)	0.0727(6)
OW3	0.4870(3)	−0.1445(4)	0.0537(1)	0.0923(9)
O1	−0.4130(2)	−0.1683(2)	0.37184(8)	0.0595(5)
O2	−0.2131(2)	0.2364(2)	−0.29961(8)	0.0613(6)
N1	−0.2961(2)	−0.1972(3)	0.13614(9)	0.0422(5)
N2	−0.0670(3)	0.4233(3)	−0.06747(9)	0.0432(5)
C11	−0.3250(2)	−0.1901(3)	0.1984(1)	0.0362(5)
C21	−0.4103(3)	−0.0769(3)	0.2163(1)	0.0504(6)
C31	−0.4373(3)	−0.0696(3)	0.2748(1)	0.0547(7)
C41	−0.3798(2)	−0.1771(3)	0.3148(1)	0.0423(5)
C51	−0.2910(3)	−0.2874(3)	0.2969(1)	0.0427(5)
C61	−0.2647(3)	−0.2945(3)	0.2383(1)	0.0432(5)
C12	−0.1031(2)	0.3768(3)	−0.12915(9)	0.0373(5)
C22	−0.0550(2)	0.4599(3)	−0.1743(1)	0.0412(5)
C32	−0.0893(2)	0.4141(3)	−0.2324(1)	0.0402(5)
C42	−0.1735(3)	0.2863(3)	−0.24411(9)	0.0416(5)
C52	−0.2219(3)	0.2051(3)	−0.1978(1)	0.0582(7)
C62	−0.1868(3)	0.2494(3)	−0.1404(1)	0.0550(7)
(b) Final atomic Coordinates for H Atoms				
H1W1	−0.245(6)	0.451(7)	0.090(3)	0.17(3)
H2W1	−0.353(6)	0.448(7)	0.118(3)	0.15(3)
H1W2	−0.382(6)	0.006(7)	0.444(2)	0.16(2)
H2W2	−0.356(6)	0.019(7)	0.502(3)	0.15(2)
H1W3	0.44(1)	−0.23(1)	0.037(5)	0.36(6)
H2W3	0.432(6)	−0.071(8)	0.059(3)	0.17(3)
H1N1	−0.224(3)	−0.130(4)	0.130(1)	0.063(9)
H2N1	−0.365(3)	−0.172(3)	0.112(1)	0.054(8)
H3N1	−0.272(3)	−0.301(4)	0.125(1)	0.058(8)
H1N2	−0.018(3)	0.514(4)	−0.066(1)	0.051(8)
H2N2	−0.005(3)	0.347(4)	−0.049(1)	0.08(1)
H3N2	−0.143(3)	0.429(4)	−0.051(1)	0.065(9)
H1	−0.367(4)	−0.244(4)	0.395(2)	0.09(1)
H2	−0.186(4)	0.296(4)	−0.323(2)	0.08(1)
H21	−0.455(3)	−0.010(3)	0.188(1)	0.059(8)
H31	−0.496(3)	0.010(4)	0.289(1)	0.073(9)
H51	−0.250(3)	−0.353(3)	0.325(1)	0.048(7)
H61	−0.205(3)	−0.363(4)	0.226(1)	0.064(9)
H22	0.006(3)	0.544(4)	−0.166(1)	0.059(8)
H32	−0.059(3)	0.469(3)	−0.265(1)	0.047(7)
H52	−0.286(3)	0.123(4)	−0.206(1)	0.08(1)
H62	−0.227(3)	0.201(4)	−0.108(1)	0.070(9)

TABLE 3
Main Interatomic Distances (Å) and Bond Angles (deg) in the $(1,4\text{-}HOC_6H_4NH_3)_4P_4O_{12}\cdot 6H_2O$ Structure

$P(1)O_4$ Tetrahedron				
P1	O11	O21	OL12	OL21
O11	**1.482(2)**	120.9(1)	106.00(9)	105.89(9)
O21	2.570(2)	**1.473(2)**	111.31(9)	111.09(9)
OL12	2.463(2)	2.539(2)	**1.601(2)**	99.37(9)
OL21	2.466(2)	2.541(2)	2.446(2)	**1.607(2)**

$P(2)O_4$ Tetrahedron				
P2	O12	O22	OL12	OL21
O12	**1.478(2)**	118.66(9)	106.43(9)	110.22(9)
O22	2.548(2)	**1.485(2)**	109.90(9)	106.29(9)
OL12	2.461(2)	2.521(2)	**1.594(2)**	104.50(9)
OL21	2.523(2)	2.467(2)	2.523(2)	**1.597(2)**

P1–P2	P1–P2	P2–P1–P2	P2–P1–P2	P1–OL12–P2	P2–OL21–P1
2.931(1) Å	2.944(1) Å	83.00(2)°	97.00(2)°	133.1(1)°	133.4(1)°

Bond Length Values in the Organic Cations (Å)

N1–C11	1.473(3)	N2–C12	1.471(3)
C11–C21	1.371(3)	C12–C22	1.372(3)
C21–C31	1.384(4)	C22–C32	1.390(3)
C31–C41	1.381(3)	C32–C42	1.386(3)
C41–C51	1.376(3)	C42–C52	1.385(3)
C51–C61	1.386(3)	C52–C62	1.376(4)
C61–C11	1.371(3)	C62–C12	1.379(3)
C41–O1	1.370(3)	C42–O2	1.356(3)
N1–H1N1	0.93(3)	N2–H1N2	0.92(3)
N1–H2N1	0.86(3)	N2–H2N2	0.97(4)
N1–H3N1	0.96(3)	N2–H3N2	0.87(3)
O1–H1	0.93(4)	O2–H2	0.81(3)
C21–H21	0.94(3)	C22–H22	0.95(3)
C31–H31	0.97(3)	C32–H32	0.95(3)
C51–H51	0.91(3)	C52–H52	0.95(3)
C61–H61	0.89(3)	C62–H62	0.96(3)

TABLE 4
Bond Lengths (Å) and Angles (deg) in the Hydrogen Bonding Scheme

O(N)–H···O	O(N)–H (Å)	H···O (Å)	O(N)···O (Å)	O(N)–H···O (deg)
N1–H1N1···O12	0.93(3)	1.90(3)	2.774(3)	155(3)
N1–H2N1···OW3 (i)	0.86(3)	1.88(3)	2.743(4)	172(3)
N1–H3N1···OW1 (i)	0.96(3)	1.96(3)	2.844(3)	152(2)
N2–H1N2···O22 (ii)	0.92(3)	1.86(3)	2.780(3)	174(2)
N2–H2N2···O21	0.97(4)	1.79(4)	2.747(3)	168(3)
N2–H3N2···OW2 (iii)	0.87(3)	2.04(3)	2.890(4)	167(3)
O1–H1···O11 (iv)	0.93(4)	1.76(4)	2.684(3)	169(4)
O2–H2···O12 (iii)	0.81(3)	1.84(4)	2.648(3)	175(4)
OW1–H1W1···O22	0.79(6)	2.07(6)	2.837(3)	166(6)
OW1–H2W1···O1 (v)	0.71(6)	2.53(6)	3.098(3)	138(6)
OW2–H1W2···O1	0.80(6)	2.22(6)	2.980(3)	158(5)
OW2–H2W2···OW1 (vi)	0.87(6)	2.17(6)	2.952(4)	150(5)
OW3–H1W3···OW2 (iv)	0.9(1)	2.0(1)	2.932(4)	160(9)
OW3–H2W3···O11	0.85(7)	1.94(7)	2.779(3)	168(6)

(i) $-1+x, y, z$; (ii) $-x, \frac{1}{2}, -y, -z$; (iii) $x, \frac{1}{2}-y, -\frac{1}{2}+z$; (iv) $x, -\frac{1}{2}+y, \frac{1}{2}-z$; (v) $-1-x, \frac{1}{2}+y, \frac{1}{2}-z$; (vi) $x, \frac{1}{2}-y, \frac{1}{2}+z$.

The B_{1u} mode of $\nu_{as}(OPO^-)$ movement, inactive in the case of D_{4h} symmetry, becomes the A_u IR-active mode in the case of C_i symmetry ($\bar{\nu} = 1260\ cm^{-1}$). The A_{2u} mode of the same movement in D_{4h} symmetry transforms to A_u mode ($\bar{\nu} = 1277\ cm^{-1}$). The frequency difference between these two bands is equal to $\Delta\bar{\nu} = 17\ cm^{-1}$. In the three frequency regions (1180–1060, 1060–960, and 850–660 cm^{-1}), the E_u modes of $\nu_s(OPO^-)$, $\nu_{as}(POP)$, and $\nu_s(POP)$ stretching vibrations split when the local symmetry of the P_4O_{12} cycle becomes C_i. The doublets resulting from this splitting are 1115–1098, 993–958, and 747–700 cm^{-1}, respectively, with $\Delta\bar{\nu} = 17\text{–}47\ cm^{-1}$ as frequency differences.

Nevertheless, one must be cautious in attribution of $\nu_{as}(OPO^-)$, $\nu_s(POP)$ vibration bands because of their possible overlapping with the ν(C–N) vibration and δ(C–H) deformation vibration bands respectively. Furthermore, the possible coupling between the P_4O_{12} cycles of the unit cell could increase the vibrational band number predicted by the theoretical group theory.

For the vibration modes in the organic cation and the deformation modes in the P_4O_{12} cycle, intensive bibliographic research (26,27) allows us to attribute easily their experimental vibration bands (Table 6).

3. *Thermal Analysis*

The simultaneously recorded differential thermal analysis and thermogravimetric analysis curves of the $(1,4\text{-}HOC_6H_4NH_3)_4P_4O_{12}\cdot 6H_2O$ compound are shown in Fig. 4.

Four endothermic peaks at 102, 228, 285, and 302°C are shown. The first peak at 102°C corresponds to the departure of four water molecules, as confirmed by weight loss detected in the TGA curve (% water: experimental, 8.49; calculated, 8.33).The second weight loss, corresponding to the two remaining water molecules, gives rise to the two endothermic peaks located at 228 and 285°C (% water: experimental, 4.12; calculated, 4.20). This loss in weight leads to the expected anhydrous salt of the cyclotetraphosphate. In fact, the analysis of the H-bond scheme (Table 4) shows that the H bonds involving the OW3 water molecule are relatively strong compared to those of OW1 and OW2. This explains the successive departure of four and two water molecules during the heating. The last peak, at 302°C, accompanied by the final important weight loss, corresponds to the organic cation degradation.

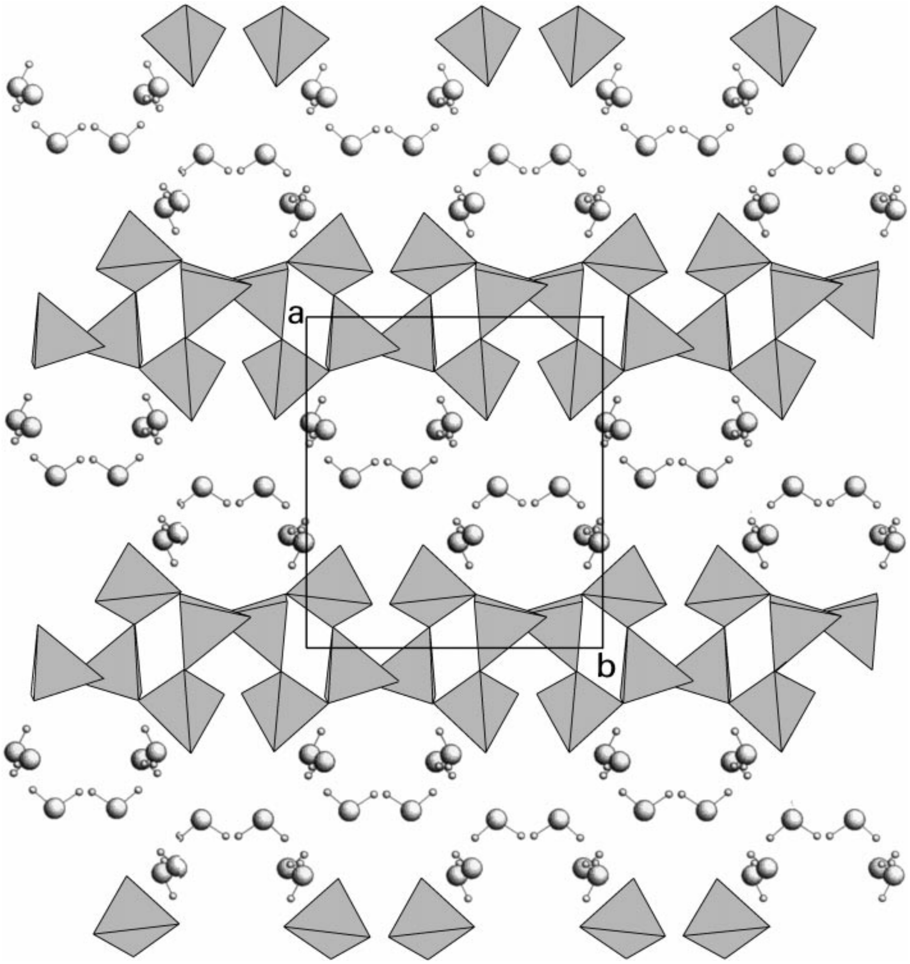

FIG. 2. Projection along the *c* axis of the P_4O_{12} groups with the water molecules.

TABLE 5
Vibrational Frequencies and Assignments in the P_4O_{12} Stretching Regions; Factor Group Analysis and Comparison with Calculated Frequencies for $(NH_4)_4P_4O_{12}$ and Experimental Frequencies for $(NH_2NH_3)_4P_4O_{12}$

			$(NH_4)_4P_4O_{12}$ (24)				$(NH_2NH_3)_4P_4O_{12}$ (25)			This work
	Molecular group		Site group		$\bar{\nu}$ (cm^{-1})		Site group		$\bar{\nu}$ (cm^{-1})	$\bar{\nu}$ (cm^{-1})
Mvt	D_{4h}	IR	C_{2h}	IR	Calc.	Obs.	C_i	IR	Obs.	Obs.
$\nu_a(OPO^-)$	A_{2u}	+	B_u	+	1272	1285	A_u	+	1280	1277 (vs)
+	B_{1u}	−	B_u	+	1241	1235	A_u	→	1235	1260 (*vs*)
$\nu(C\text{–}N)$	E_g	−	A_g	−			A_g	−		
			B_g	−			A_g	−		
	A_{1g}	−	A_g	−	1272	1285	A_g	−		
$\nu_s(OPO^-)$	B_{2g}	−	B_g	−	1241	1235	A_g	−		
	E_u	+	A_u	+	1128	1102	A_u	+	1135	1115 (vs)
			B_u	+	1087		A_u	+	1100	1098 (vs)
	A_{2g}	−	B_g	−	1272	1285	A_g	−		
$\nu_a(POP)$	B_{2g}	−	A_g	−	1241	1235	A_g	−		
	E_u	+	B_u	+	993	987	A_u	+	1000	993 (s)
			A_u	+	982		A_u	+	985	958 (vs)
$\nu_s(POP)$	A_{1g}	−	A_g	−		1285	A_g	−		
+	B_{1g}	−	B_g	−		1235	A_g	−		
$\delta(C\text{–}H)$	E_u	+	B_u	+	752	738	A_u	+	745	747 (s)
			A_u	+	689	693	A_u	+	700	700 (s)

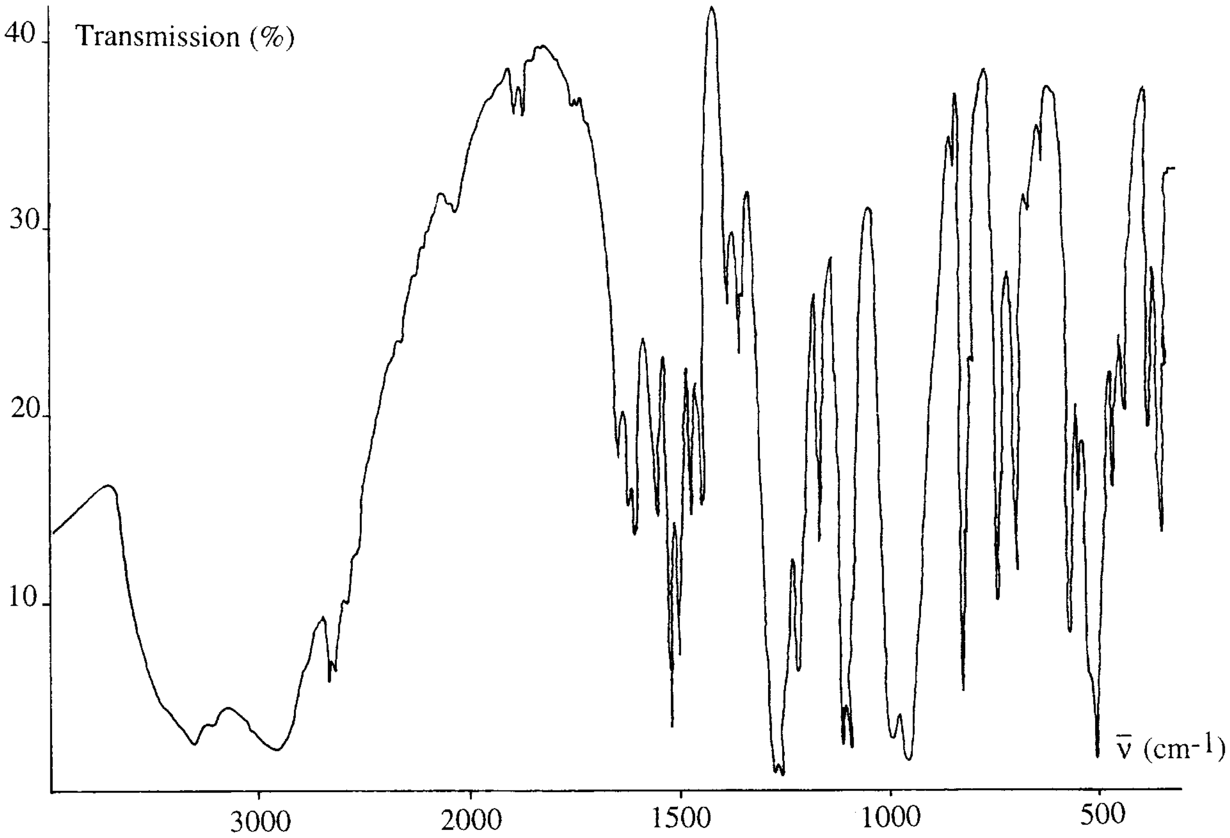

FIG. 3. IR spectrum of $(1,4\text{-}HOC_6H_4NH_3)_4P_4O_{12} \cdot 6H_2O$ phosphate at 300 K.

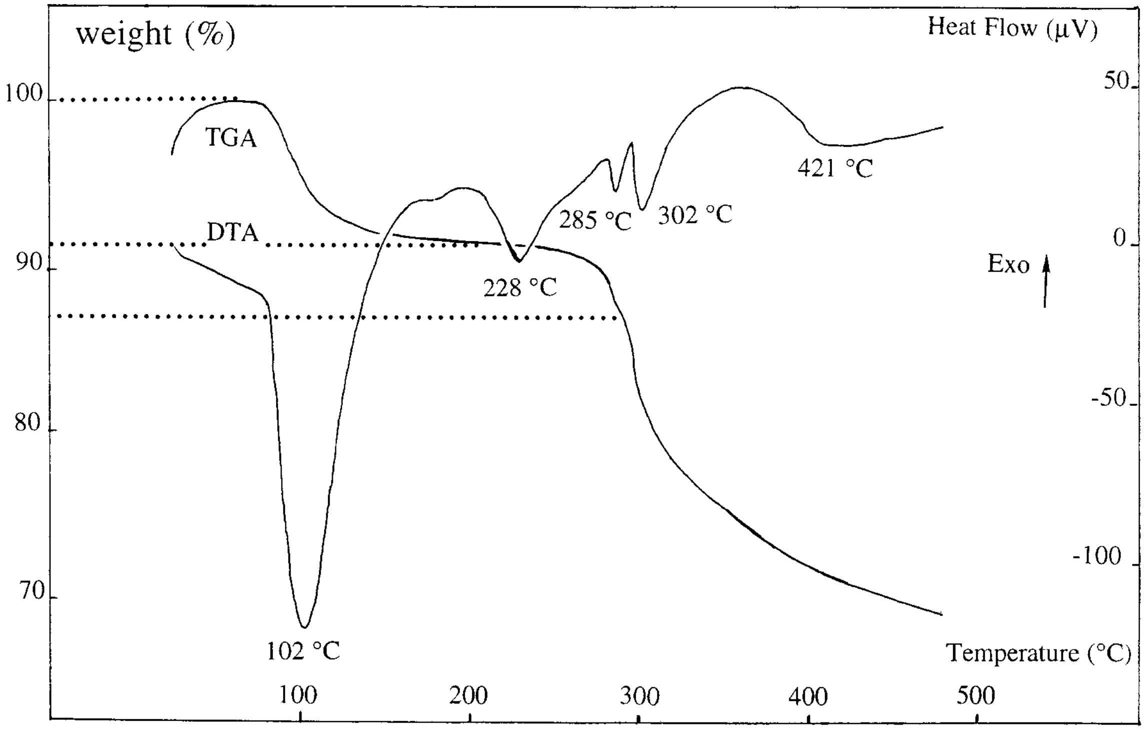

FIG. 4. TG-DTA thermograms of the $(1,4\text{-}HOC_6H_4NH_3)_4P_4O_{12} \cdot 6H_2O$ phoaphate.

TABLE 6
Tentative Assignments of the Observed IR Frequencies Outside the Stretching Domain of P_4O_{12} Rings

$\bar{\nu}$ (cm^{-1})	Attributions	$\bar{\nu}$ (cm^{-1})	Attributions
3112 (w)	$\nu(NH_3^+)$	1223 (s)	ν(C–O)
3065 (w)	+ ν(C–H)	1172 (s)	+ ν(C–N)
2914 (b)	+ $\nu(OH_2)$	860 (w)	+
2666 (m)	+ $\nu(OH)_{ph.}$	826 (s)	δ(C–H) in plan
1834 (w)	Combination	666 (w)	δ(C–H) out plan
1878 (w)	bands[a]	650 (w)	+ $\delta(O–H)_{ph}$. out plan
1648 (m)	$\delta(NH_3^+)$	574 (s)	
1628 (w)	+	551 (m)	
1610 (m)	$\delta(OH_2)$	510 (s)	Deformation
1554 (m)	+	472 (m)	vibrations
1521 (s)	$\delta(OH)_{ph.}$	446 (m)	+
1503 (s)	+	386 (m)	External
1473 (m)	ν(C=C) of	358 (s)	modes
1455 (m)	the organic	–	
1386 (m)	cation	–	
1362 (m)		–	

[a] Combination bands between C–H out of plane: w, weak; m, medium; b, broad; s, strong.

REFERENCES

1. A. Durif and M. T. Averbuch-Pouchot, *Acta Crystallogr. Sect. C* **45,** 1884 (1989).
2. A. Durif and M. T. Averbuch-Pouchot, *Acta Crystallogr. Sect. C* **46,** 2026 (1990).
3. M. T. Averbuch-Pouchot and A. Durif, *Eur. J. Solid State Inorg. Chem.* **29,** 411 (1992).
4. M. T. Averbuch-Pouchot, A. Durif, and J. C. Guitel, *Acta Crystallogr. Sect. C* **44,** 1416 (1998).
5. J. L. Isabev, A. Ibragimov, S. A. Talipov, M. T. Saibova, and T. F. Aripov, *Russ. J. Inorg. Chem.* **26,** 1086 (1982).
6. J. M. Adams and V. Ramdas, *Acta Crystallogr Sect. B* **33,** 3654 (1977).
7. E. H. Soumhi and T. Jouini, *Acta Crystallogr. Sect. C* **51,** 1883 (1995).
8. E. H. Soumhi and T. Jouini, *Acta Crystallogr. Sect. C* **51,** 1457 (1995).
9. E. H. Soumhi and T. Jouini, *Acta Crystallogr. Sect. C* **52,** 432 (1996).
10. E. H. Soumhi and T. Jouini, *Acta Crystallogr. Sect. C* **52,** 2802 (1996).
11. M. Casciola, U. Costantino, and S. D'Amico, *Solid State Ionics* **22,** 17 (1986).
12. J. Zyss, *in* "Conjugated Polymeric Materials: Opportunities in Electronics" (J. L. Brédas and R. R. Chance, Eds.), Optoelectronics and Molecular Electronics, p. 545. Kluwer, Dordrecht, 1990.
13. R. Masse, M. Bagieu-Beucher, J. Pecault, J. P. Levy, and J. Zyss, *Nonlinear Opt*. **5,** 413 (1993).
14. G. Alberti, M. Casciola, U.Costantino, and R. Radi, *Gazz. Chim. Ital.* **109,** 412 (1979).
15. G. Alberti, M. Bracardi, and M. Casciola, *Solid State Ionics* **7,** 243 (1982).
16. A. Durif, "Crystal Chemistry of Condensed Phosphates." Plenum, London, 1995.
17. J. M. Pollock and M. Soharan, *J. Chim. Phys.* **51,** 3604 (1969).
18. H. Thabet, A. Jouini, and E. H. Soumhi, *Acta Crystallogr. Sect C* **53,** 318 (1997).
19. E. H. Soumhi, A. Driss, and T. Jouini, *Mater. Res. Bull.* **29**(7), 767 (1994).
20. E. H. Soumhi and T. Jouini, *Acta Crystallogr. Sect. C* **51,** 1213 (1995).
21. E. H. Soumhi and T. Jouini, *Acta Crystallogr. Sect. C* **52,** 434 (1996).
22. R. H. Blessing, *Acta Crystallogr. Sect. C* **42,** 613 (1986).
23. I. D. Brown, *Acta Crystallogr. Sect. A* **32,** 24 (1976).
24. K. K. Muldagaliev, A. N. Lazarev, and A. P. Mirgorodskii, *Izv. Akad. Nauk. SSSR, Neorg. Mater.* **10**(4), 661 (1974).
25. H. Thabet, M. Bdiri, A. Jouini, and A. Durif, *J. Solid State Chem.* **101,** 211 (1992).
26. K. Larafa, A. Mahjoub, M. Rzaigui, and A. Durif, *Eur. J. Solid State Inorg. Chem.* **34,** 481 (1997).
27. Josien and Lebas, *Bull. Soc. Chim. Fr*. **53,** 57 (1956).
28. Enraf–Nonius, "CAD-4 Software, Version 5.0." Enraf–Nonius, Delft, 1989.
29. C. K. Fair, "MolEN, An Interactive Intelligent System for Crystal Structure Analysis." Enraf–Nonius, Delft, 1990.
30. G. M. Sheldrick, *Acta Crystallogr. Sect. A* **46,** 467 (1990).
31. G. M. Sheldrick, "SHELXL93, Program for the Refinement of Crystal Structures." University of Göttingen, 1993.